AIAA JOURNAL
Vol. 41, No. 11, November 2003

Lamination Parameters Applied to Reliability-Based In-Plane Strength Design of Composites

Nozomu Kogiso* and Shuuya Nakagawa†
Osaka Prefecture University, Sakai, Osaka 599-8531, Japan
and
Yoshisada Murotsu‡
Osaka Prefectural College of Technology, Neyagawa, Osaka 572-8572, Japan

The efficiency of adopting lamination parameters as design variables for the reliability-based optimization of a laminated composite plate subject to in-plane loads is presented. The plate failure is evaluated by the first-ply failure (FPF) criterion, where the ply failure is evaluated based on the Tsai–Wu criterion. According to the FPF criterion, the laminated plate is modeled as a series system consisting of every ply failure. The system reliability of the composite plate is evaluated by Ditlevsen's bounds. Each ply-failure probability is evaluated by the first-order reliability method, where the material properties and applied loads are treated as random variables. As numerical examples, two types of the reliability-based design are formulated in terms of lamination parameters. One is the reliability-maximized design of the constant-thickness plate. The other is the thickness-minimized design under the reliability constraint. Through numerical calculations, it is shown that the reliability has a single peak and a continuous distribution in the lamination parameter space. Consequently, numerical searching rapidly achieves the optimum solution.

Introduction

LAMINATED composite plates are widely used in structural applications because of their high specific strength and stiffness. Therefore, many studies have been conducted on the optimum design of laminated composite plates by changing their laminate constructions.[1] However, most of them yield the optimum laminate constructions under deterministic conditions, where the material properties and the loading conditions are assumed to have no variations. It has been known that such a deterministic optimum design is strongly anisotropic and sensitive to change in loading conditions. Therefore, it is necessary to consider the effect of such variations by applying the structural reliability theory.[2] For structural safety, an optimum laminate configuration design considering the reliability is important.

The reliability-based design under the in-plane strength via the first-ply failure (FPF) criterion was already studied.[3–5] The studies have shown that the reliability increases as the number of fiber axes is increased, and that the reliability-based design approaches a quasi-isotropic configuration. The design is much different from the deterministic optimum design for which the orientation angle runs along the loading direction.

The reliability is commonly evaluated by the first-order reliability method (FORM),[2] which is formulated as a nonlinear programming problem for a nonlinear limit state function. Accordingly, the reliability-based optimization problem is formulated as a nested optimization problem and, hence, it takes much computational time. Therefore, significantly improving the calculation efficiency is difficult.

For a deterministic laminate construction design problem, lamination parameters were introduced.[6] When the laminate construction is balanced symmetric, the in-plane mechanical properties are described by only two in-plane lamination parameters with weak nonlinearity. Additionally, the laminate construction can be determined easily from the lamination parameter values. Therefore, the lamination parameters have been applied as design variables of several optimum design problems.[1,7]

Accordingly, adopting the lamination parameters as design variables is considered a good strategy for the reliability-based design. The first study of the lamination parameters applied to the reliability-based design was made for in-plane stiffness or stiffness-related properties.[8] The study clarified the distribution of in-plane stiffness variation in the lamination parameter space, where the material properties have variations.

This study will make more active use of the lamination parameters for the reliability-based optimization. Specifically, two types of the reliability-based in-plane strength design problems are formulated in terms of lamination parameters to improve the calculation efficiency. One is the reliability-maximized design of the constant-thickness plate. The other is the thickness-minimized design under the reliability constraint. For a balanced symmetric laminated plate consisting of 0-, ±45-, and 90-deg plies, the plate failure is determined by the FPF criterion, where the ply failure is evaluated based on the Tsai–Wu criterion.[9] According to the FPF criterion, the laminated plate is modeled as a series system consisting of every ply failure. The system reliability of the composite plate is evaluated by Ditlevsen's bounds.[10] As a system component, the ply-failure probability is evaluated by the FORM, where the material properties and applied loads are treated as random variables.

Through numerical calculations, it is clarified that the reliability has a single peak and continuous distribution in the lamination parameter space. Then the efficiency of adopting the lamination parameters as design variables is demonstrated.

Laminated Composite Plate

A balanced symmetric laminated plate is considered, shown in Fig. 1, that is made of a single fibrous material subject to in-plane loads. The in-plane and flexural responses can be separated for the symmetric layup condition and also the in-plane extension–shear coupling cannot happen. Accordingly, only the in-plane stress–strain relationship is considered. The in-plane strain $\epsilon = (\epsilon_1, \epsilon_2, \epsilon_6)^T$

Presented as Paper 2002-5562 at the AIAA/ISSMO 9th Symposium on Multidisciplinary Analysis and Optimization, Atlanta, GA, 4 September 2002; received 3 April 2003; revision received 15 June 2003; accepted for publication 20 June 2003.

*Associate Professor, Department of Aerospace Engineering; kogiso@aero.osakafu-u.ac.jp. Member AIAA.
†Graduate Student, Department of Aerospace Engineering.
‡President. Senior Member AIAA.

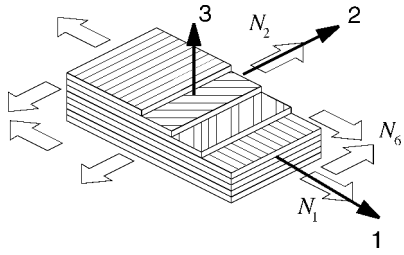

Fig. 1 Symmetric laminated composite plate.

is obtained by the following constitutive equation:

$$\begin{Bmatrix} N_1 \\ N_2 \\ N_6 \end{Bmatrix} = \begin{bmatrix} A_{11} & A_{12} & 0 \\ A_{12} & A_{22} & 0 \\ 0 & 0 & A_{66} \end{bmatrix} \begin{Bmatrix} \epsilon_1 \\ \epsilon_2 \\ \epsilon_6 \end{Bmatrix} \tag{1}$$

where $(N_1, N_2, N_6)^T$ denotes the stress resultant and the matrix $\boldsymbol{A}$ is the in-plane stiffness of the balanced symmetric laminate. The subscripts 1, 2, and 6 correspond to the longitudinal, lateral, and in-plane shear directions, respectively, as shown in Fig. 1.

The ply strain along the material principal direction $(\epsilon_x, \epsilon_y, \epsilon_s)^T$ with ply orientation angle θ is obtained through the plate strain transformation as follows:

$$\begin{Bmatrix} \epsilon_x \\ \epsilon_y \\ \epsilon_s \end{Bmatrix} = \begin{bmatrix} \cos^2\theta & \sin^2\theta & \cos\theta\sin\theta \\ \sin^2\theta & \cos^2\theta & \cos\theta\sin\theta \\ -2\cos\theta\sin\theta & 2\cos\theta\sin\theta & \cos^2\theta - \sin^2\theta \end{bmatrix} \begin{Bmatrix} \epsilon_1 \\ \epsilon_2 \\ \epsilon_6 \end{Bmatrix} \tag{2}$$

where x, y, and s correspond to the major and minor axes and shear directions, respectively, along the material principal directions. The ply stress along the material principal direction $(\sigma_x, \sigma_y, \sigma_s)^T$ is obtained from the following equation:

$$\begin{Bmatrix} \epsilon_x \\ \epsilon_y \\ \epsilon_s \end{Bmatrix} = \begin{bmatrix} Q_{xx} & Q_{xy} & 0 \\ Q_{xy} & Q_{yy} & 0 \\ 0 & 0 & Q_{ss} \end{bmatrix} \begin{Bmatrix} \sigma_x \\ \sigma_y \\ \sigma_s \end{Bmatrix} \tag{3}$$

where Q_{xx}, Q_{yy}, Q_{xy}, and Q_{ss} are the ply stiffness terms. These terms are described in terms of four independent engineering material constants, Young's modulus along the fiber direction E_x, Young's modulus transverse to the fiber direction E_y, in-plane shear modulus E_s, and Poisson's ratio ν_x as follows:

$$Q_{xx} = \frac{E_x^2}{\left(E_x - \nu_x^2 E_y\right)}, \qquad Q_{yy} = \frac{E_x E_y}{\left(E_x - \nu_x^2 E_y\right)}$$

$$Q_{xy} = \frac{\nu_x E_x E_y}{\left(E_x - \nu_x^2 E_y\right)}, \qquad Q_{ss} = E_s \tag{4}$$

Lamination Parameters

Using the lamination parameters, the in-plane stiffness terms A_{ij} can be described by the material stiffness and the laminate construction terms separately[6]:

$$\begin{Bmatrix} A_{11} \\ A_{22} \\ A_{12} \\ A_{66} \end{Bmatrix} = h \begin{bmatrix} U_1 & V_1^* & V_2^* \\ U_1 & -V_1^* & V_2^* \\ U_4 & 0 & -V_2^* \\ U_5 & 0 & -V_2^* \end{bmatrix} \begin{Bmatrix} 1 \\ U_2 \\ U_3 \end{Bmatrix} \tag{5}$$

where (V_1^*, V_2^*) are called lamination parameters determined by laminate construction, $U_i (i = 1, \ldots, 5)$ are material invariants, and h is the total plate thickness.

The material invariants U_i are described by the ply elastic constants $\boldsymbol{Q}$:

$$\begin{Bmatrix} U_1 \\ U_2 \\ U_3 \\ U_4 \\ U_5 \end{Bmatrix} = \frac{1}{8} \begin{bmatrix} 3 & 3 & 2 & 4 \\ 4 & -4 & 0 & 0 \\ 1 & 1 & -2 & -4 \\ 1 & 1 & 6 & -4 \\ 1 & 1 & -2 & 4 \end{bmatrix} \begin{Bmatrix} Q_{xx} \\ Q_{yy} \\ Q_{xy} \\ Q_{ss} \end{Bmatrix} \tag{6}$$

The lamination parameters (V_1^*, V_2^*) are defined in terms of the ply orientation angle $\pm\theta_i$ and the volume fraction v_i as follows:

$$V_1^* = \sum_{i=1}^{N} v_i \cos 2\theta_i, \qquad V_2^* = \sum_{i=1}^{N} v_i \cos 4\theta_i \tag{7}$$

where N is the number of different ply angle groups,

$$v_1 + v_2 + \cdots + v_N = 1 \tag{8}$$

The feasible region of the lamination parameters of the balanced symmetric laminate is defined by the following inequalities[6]:

$$V_2^* \geq 2V_1^{*2} - 1, \qquad V_2^* \leq 1 \tag{9}$$

Any point inside this feasible region must correspond to laminates with two or more ply orientation angles.

For a symmetric angle-ply laminate with only one ply orientation angle, $[\pm\theta]_s$, where the subscript s denotes the symmetric laminate configuration with respect to the midplane, the lamination parameters, $(V_1^*, V_2^*) = (\cos 2\theta, \cos 4\theta)$, lie on the following parabola as shown in Fig. 2:

$$V_2^* = 2V_1^{*2} - 1 \tag{10}$$

which is easily obtained from a trigonometric function law.

When the symmetric balanced laminate consists of three kinds of ply orientation, the feasible region of the lamination parameters is inside of a triangle, where the three vertices are located on the parabola of the corresponding ply angle. Accordingly, when the ply orientation angles are limited to 0, ±45, and 90 deg, the feasible region of the lamination parameter space is described by the following inequalities:

$$V_2^* \geq 2V_1^* - 1, \qquad V_2^* \geq -2V_1^* - 1, \qquad V_2^* \leq 1 \tag{11}$$

where the three vertices (1, 1), (0, −1), and (−1, 1) correspond to 0, ±45, and 90 deg, respectively. The feasible triangle is illustrated as the shaded area in Fig. 2.

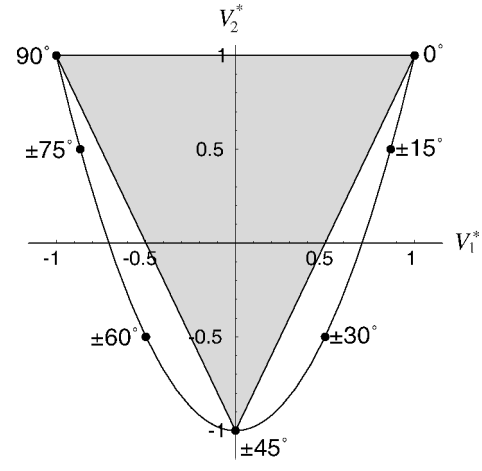

Fig. 2 Lamination parameter space of symmetric balanced laminate; the shading indicates the feasible region of $[0, \pm 45, 90]_s$ laminate.

Strength Analysis

The ply strength is evaluated via the Tsai–Wu criterion.[9] The failure envelope is described as an ellipsoid in the stress space:

$$F_{xx}\sigma_x^2 + 2F_{xy}\sigma_x\sigma_y + F_{yy}\sigma_y^2 + F_{ss}\sigma_s^2 + F_x\sigma_x + F_y\sigma_y - 1 = 0 \quad (12)$$

where material strength parameters F_{xx}, F_{yy}, F_{xy}, F_{ss}, F_x, and F_y are defined by the material strengths as follows:

$$F_{xx} = 1/(X_t X_c), \qquad F_{yy} = 1/(Y_t Y_c)$$

$$F_{xy} = F_{xy}^*(F_{xx}F_{yy})^{\frac{1}{2}}, \qquad F_{ss} = 1/S^2$$

$$F_x = 1/X_t - 1/X_c, \qquad F_y = 1/Y_t - 1/Y_c \quad (13)$$

where X_t and X_c are the tensile and compressive strengths along the fiber direction, respectively; Y_t and Y_c are the tensile and compressive strengths perpendicular to the fiber direction, respectively; and S is a shear strength; F_{xy}^* is the correlation constant between each strength parameter and is set to -0.5.

In this study, the Tsai–Wu criterion in the strain space is adopted because of the calculation efficiency of the reliability analysis.[11] The Tsai–Wu criterion in the strain space is described as

$$G_{xx}\epsilon_x^2 + 2G_{xy}\epsilon_x\epsilon_y + G_{yy}\epsilon_y^2 + G_{ss}\epsilon_s^2 + G_x\epsilon_x + G_y\epsilon_y - 1 = 0 \quad (14)$$

where the strength parameters in the strain space G_{xx}, G_{yy}, G_{xy}, G_{ss}, G_x, and G_y are obtained by substituting the ply stress–strain relationship (3) into Eq. (12) as follows:

$$G_{xx} = F_{xx}Q_{xx}^2 + 2F_{xy}Q_{xx}Q_{xy} + F_{yy}Q_{xy}^2$$

$$G_{yy} = F_{xx}Q_{xy}^2 + 2F_{xy}Q_{xy}Q_{yy} + F_{yy}Q_{yy}^2$$

$$G_{xy} = F_{xx}Q_{xx}Q_{xy} + F_{xy}\left(Q_{xx}Q_{yy} + Q_{xy}^2\right) + F_{yy}Q_{xy}Q_{yy}$$

$$G_{ss} = F_{ss}Q_{ss}^2, \qquad G_x = F_xQ_{xx} + F_yQ_{xy}$$

$$G_y = F_xQ_{xy} + F_yQ_{yy} \quad (15)$$

Strength Ratio

The strength ratio R_i is defined as the ratio between the ply failure strain $\boldsymbol{\epsilon}_F$ and the ith ply strain $\boldsymbol{\epsilon}_i = (\epsilon_x, \epsilon_y, \epsilon_s)_i^T$ under the proportional loading assumption[9]:

$$\boldsymbol{\epsilon}_F = R_i\boldsymbol{\epsilon}_i \quad (16)$$

The ply-strength ratio R_i is evaluated by solving the following quadratic equation obtained by substituting Eq. (16) into Eq. (14):

$$\left(G_{xx}\epsilon_x^2 + 2G_{xy}\epsilon_x\epsilon_y + G_{yy}\epsilon_y^2 + G_{ss}\epsilon_s^2\right)R_i^2 + (G_x\epsilon_x + G_y\epsilon_y)R_i - 1 = 0 \quad (17)$$

In this study, the FPF criterion is adopted. That is, the plate strength ratio is represented by the smallest ply strength ratio:

$$R_{\min} = \min_i R_i \quad (18)$$

The plate is considered a failure when $R_{\min}$ is less than unity as shown in Fig. 3.

Reliability Analysis

The reliability subject to the FPF criterion is evaluated by modeling the plate failure as a series system consisting of every ply failure, where the material constants and the applied loads are treated as random variables.

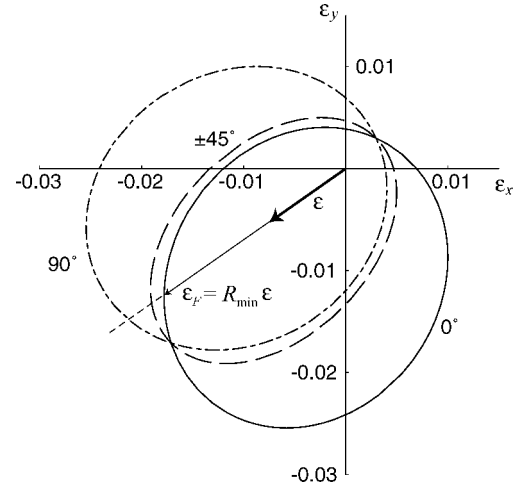

Fig. 3 Failure envelopes of $[0, \pm 45, 90]_s$ laminate in the strain space.

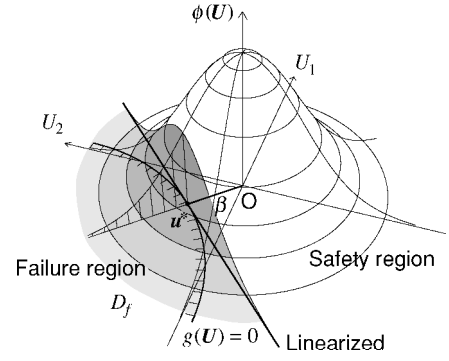

Fig. 4 First-order reliability method (FORM).

Ply-Failure Probability

The reliability of each ply failure is evaluated by FORM.[2] The limit state function of the ith ply is defined as follows:

$$g_i(\boldsymbol{z}) = h_i(\boldsymbol{u}) = R_i - 1 \begin{cases} > 0 & \text{safety} \\ = 0 & \text{limit state} \\ < 0 & \text{failure} \end{cases} \quad (19)$$

where R_i is the strength ratio of the ith ply defined in Eq. (17) and $\boldsymbol{u}$ is a random vector transformed into the standardized normal distribution space ($\boldsymbol{U}$ space) from the original random variable $\boldsymbol{z}$.

The reliability index is evaluated through the following nonlinear programming problem:

$$\text{Minimize: } \beta_i = \sqrt{\boldsymbol{u}^T\boldsymbol{u}}, \qquad \text{subject to: } h_i(\boldsymbol{u}) = 0 \quad (20)$$

As shown in Fig. 4, the limit state function is linearized at the design point. Then the failure probability is evaluated by using a standardized normal distribution function:

$$P_i = \Phi(-\beta_i) = \int_{-\infty}^{-\beta_i} \frac{1}{\sqrt{2\pi}} \exp\left(-\frac{x^2}{2}\right) \mathrm{d}x \quad (21)$$

It is known that problem (20) has multiple local optima, because limit state function (19) is strongly nonlinear. Premature convergence will yield the overestimation of the reliability. To avoid the premature convergence, a global optimization method should be recommended for the numerical searching. In this study, the modified tunneling method suitable for the FORM developed by the authors[12] is utilized as one of the global optimization methods. The tunneling algorithm[13] and the modified tunneling function for the FORM are described in the Appendix.

System Reliability

The plate system is modeled as a series system consisting of each ply failure. The system reliability is approximated by Ditlevsen's bounds[10]:

$$P_L \le P_s \le P_U, \qquad P_L = P_1 + \sum_{i=2}^{m} \max\left(P_i - \sum_{j=1}^{i-1} P_{ij}, 0 \right)$$

$$P_U = \sum_{i=1}^{m} P_i - \sum_{i=2}^{m} \max_{j<i} P_{ij} \tag{22}$$

where P_i is the ith ply failure probability and P_{ij} is the joint probability of the ith and jth ply failures; m is the number of failure modes, which is set to 4 for the symmetric balanced laminate consisting of 0-, ±45-, and 90-deg plies.

The reliability indices of the lower and the upper bounds are evaluated by using the inverse of the standardized normal distribution function:

$$\beta_U \le \beta_s \le \beta_L, \qquad \beta_L = -\Phi^{-1}(P_L), \qquad \beta_U = -\Phi^{-1}(P_U) \tag{23}$$

The reliability index β_U corresponding to the upper limit P_U is regarded as the system reliability index.

Numerical Examples

As numerical examples, a symmetric balanced laminated composite plate consisting of 0-, ±45-, and 90-deg plies with the plate size of 0.1×0.1 m^2 and 1.0 mm thickness is used. The material properties are assumed to be normally distributed, where the means and coefficients of variation are listed in Table 1. Two applied-load cases with normal distribution are considered, where the means and standard deviations are listed in Table 2.

The objective is to demonstrate the effectiveness of adopting lamination parameters as design variables on the reliability-based optimization. At first, it is demonstrated that the reliability has a single peak and continuous distribution in the lamination parameter space. Then the FORM is confirmed to have enough accuracy for the optimization in comparison with crude Monte Carlo simulation. Additionally, it is demonstrated that the continuous reliability distribution in the lamination parameter space is obtained for the other types of random distribution, because assumption of the normal distribution is not always correct for practical situation. Finally, the efficiency of adopting the lamination parameters as design variables is demonstrated for two types of reliability-based optimization.

Table 1 Material properties of T300/5208

Random variable	Mean	COV[a]
E_x, GPa	181.0	0.05
E_y, GPa	10.3	0.05
E_s, GPa	7.17	0.05
ν_x	0.28	0.01
X_t, MPa	1500.0	0.1
X_c, MPa	1500.0	0.1
Y_t, MPa	40.0	0.1
Y_c, MPa	246.0	0.1
S, MPa	68.0	0.1

[a]Coefficient of variation.

Table 2 Loading conditions

	Load case 1		Load case 2	
Stress resultant	Mean	SD[a]	Mean	SD
N_1 (MN/m)	0.1	0.03	0.1	0.03
N_2 (MN/m)	0.1	0.03	0.05	0.03
N_6 (MN/m)	0.0	0.03	0.04	0.03

[a]Standard deviation.

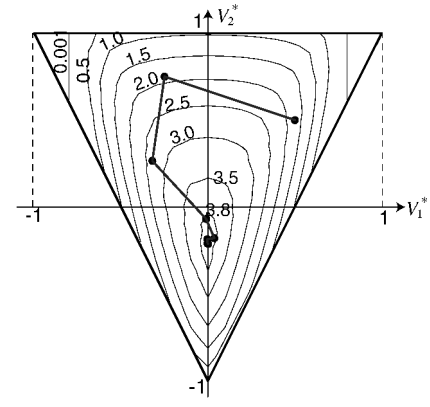

a) Load case 1

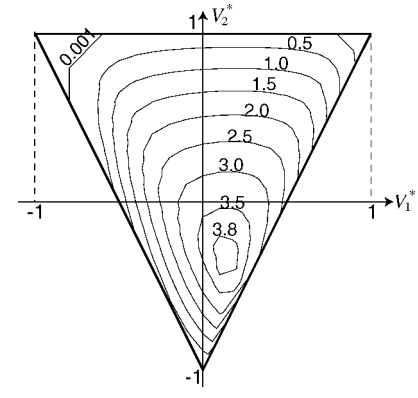

b) Load case 2

Fig. 5 Reliability distribution in lamination parameter space.

Reliability Distribution

At first, the reliability distribution in the lamination parameter space is investigated. The reliability contour curves for both load cases are illustrated in Fig. 5. These contour plots are drafted from the reliability evaluations by the FORM at 221 grid points with every 0.1 spacing in the lamination parameter space. It is found that the reliability has a single peak and a continuous distribution in the lamination parameter space. This fact implies that adopting the lamination parameters as design variables will be a good strategy for the reliability-based optimization.

Confirmation by Monte Carlo Simulation

The accuracy of the FORM is confirmed by comparing with the crude Monte Carlo simulation. In the Monte Carlo simulation, the reliability index is evaluated via 10^7 iterations of random analyses at the 221 lattice points. The reliability contour for both load cases are illustrated in Fig. 6, where the solid curves are drawn from the Monte Carlo simulation results and the dotted curves are from the FORM of Fig. 5.

Additionally, the obtained results at near-optimum designs are compared in Table 3. The coefficient of variation on the estimated failure probability, $\widehat{\mathrm{COV}}(P_f)$ is sufficiently small, which means that the failure probability obtained by the Monte Carlo simulation is close to the true value.

Because $\widehat{\mathrm{COV}}(P_f)$ at the points with smaller reliability is usually smaller than that at this point, the Monte Carlo simulation is accurate enough in the whole lamination parameter space. This implies that the FORM would overestimate the reliability. More accurate reliability would be obtained by using a higher order analysis such as the second-order reliability method.[2] However, it takes additional computational time after obtaining the reliability index. Because the reliability obtained by the FORM is almost identical to that by the Monte Carlo simulation as shown in Fig. 6, adopting the FORM is reasonable for the reliability-based optimization.

Table 3 Comparison between FORM and Monte Carlo simulation

	Load case 1, $(V_1^*, V_2^*) = (0.0, -0.2)$			Load case 2, $(V_1^*, V_2^*) = (0.1, -0.3)$		
Simulation	β	P_f	$\widehat{\mathrm{COV}}(P_f)$[a]	β	P_f	$\widehat{\mathrm{COV}}(P_f)$
Monte Carlo	3.867	5.52×10^{-5}	0.0426	3.834	6.31×10^{-5}	0.0398
FORM	3.927	4.29×10^{-5}	——	3.910	4.61×10^{-5}	——

[a] Coefficient of variation on the failure probability.

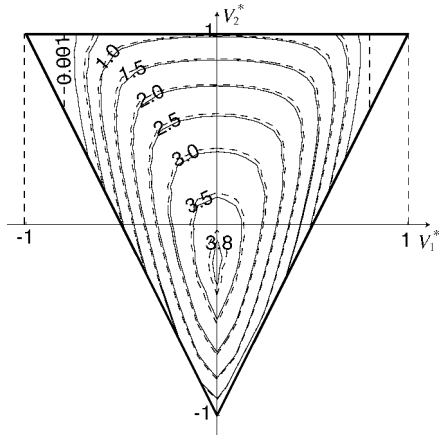

a) Load case 1

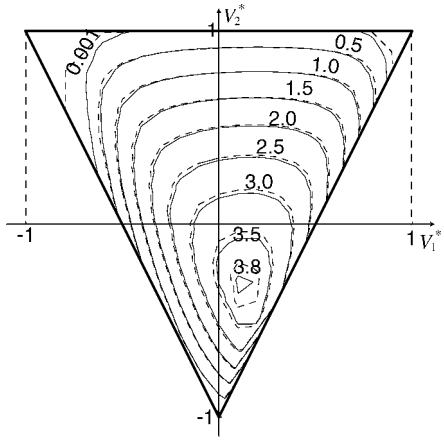

b) Load case 2

Fig. 6 Comparison of reliability distributions between Monte Carlo simulation (solid curves) and FORM (dotted curves).

Effect of Probabilistic Distribution Type

Assumption of normal distribution is not always correct for practical situations. Therefore, the other types of distribution type, log-normal and Weibull distributions, are investigated. These distributions as well as normal distributions are often used for structural reliability models.

Figure 7 shows reliability contour plots of load case 2 in the lamination parameter space under the case where the material properties are assumed to have log-normal or Weibull distributions with the same means and coefficients of variation as Table 1. On the other hand, the applied loads are assumed to have the same normal distribution as the preceding examples. The plots show that the distribution types have large effects on the reliability index value and, hence, the reliability-maximized point will be shifted. However, the reliability has continuous and single-peak distributions in the lamination parameter space regardless of distribution types. This implies that the lamination parameter is useful as a design variable for the reliability-based optimization.

Reliability Maximization

The reliability is maximized in the lamination parameter space for the laminated plate with constant thickness of 1.0 mm.

Table 4 Reliability-maximized design.

Parameter	Load case 1	Load case 2
V_1^*	0.0	0.139
V_2^*	−0.212	−0.358
β_{opt}	3.927	3.956
h_0, mm	0.197	0.230
$h_{\pm 45}$, mm	0.606	0.679
h_{90}, mm	0.197	0.091

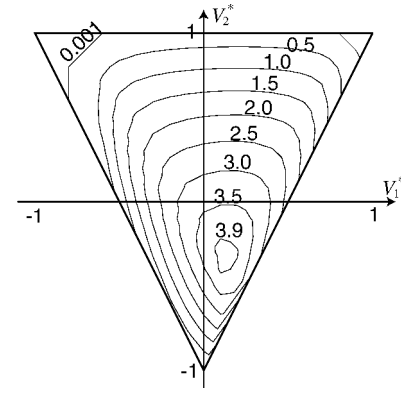

a) Log-normal distribution

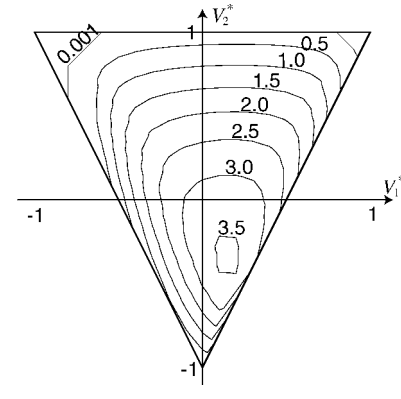

b) Weibull distribution

Fig. 7 Reliability contour for other probabilistic distribution types in load case 2.

The convergence process of load case 1 from the initial design $(V_1^*, V_2^*) = (0.5, 0.5)$ is overplotted in Fig. 5a. The path shows that the optimization run converges to the optimum design smoothly.

The obtained optimum designs are listed in Table 4. The ply thickness is obtained through the definition of the lamination parameters as follows:

$$v_0 - v_{90} = V_1^*, \qquad v_0 - v_{45} + v_{90} = V_2^*, \qquad v_0 + v_{45} + v_{90} = 1 \tag{24}$$

In both cases, the optimum designs are located inside of the feasible regions, which require all of the ply orientation angles, 0, ±45, and 90 deg. This is in good contrast with the deterministic optimum design, which is located at the boundary of the lamination parameter

Table 5 Thickness-minimized design

Parameter	Load case 1	Load case 2
V_1^*	0.0	0.156
V_2^*	−0.204	−40.356
h_{opt}, mm	0.821	0.814
h_0, mm	0.163	0.195
$h_{\pm 45}$, mm	0.495	0.552
h_{90}, mm	0.163	0.067

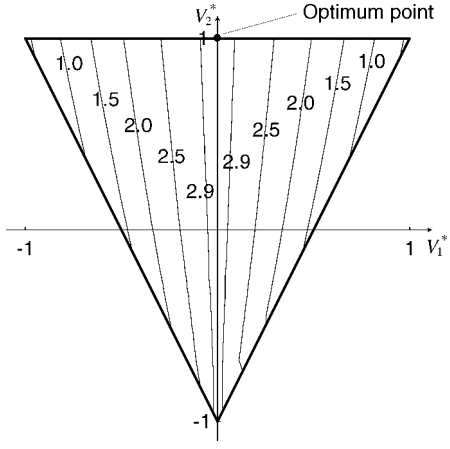

a) Load case 1

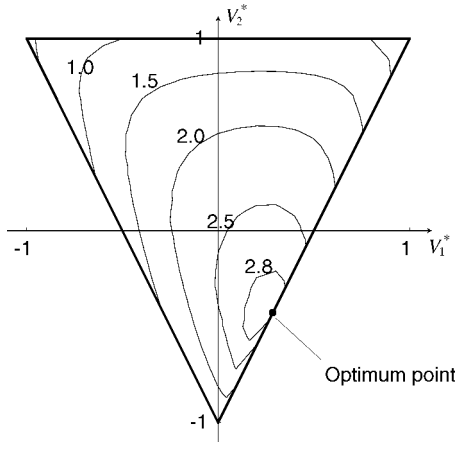

b) Load case 2

Fig. 8 Strength ratio distribution under the mean applied load.

space and hence consists of only two kinds of ply orientation angles, as shown in Fig. 8.

Thickness Minimization

The plate thickness is minimized under the reliability constraint, $\beta_U \leq 3.0$, where the plate thickness is treated as a design variable in addition to the lamination parameters.

The convergence history for load case 2 is shown in Fig. 9. It is found that the searching reaches convergence smoothly. The searching is started from $(V_1^*, V_2^*) = (0.5, 0.5)$ with the plate thickness of 1.0 mm. At the early stage, the plate thickness is decreased, but the reliability is improved by moving the lamination parameter value from the initial violated design. Then the searching reaches near-optimum design by four iterations.

The optimum designs for both cases are listed in Table 5. The optimum lamination parameter values and, hence, the optimum laminate constructions are very similar to the reliability-maximized design in Table 4.

Finally, the reliability contour at the optimum thickness is shown in Fig. 10. It shows that any design except for the obtained point has lower reliability and, hence, the obtained result is a true optimum.

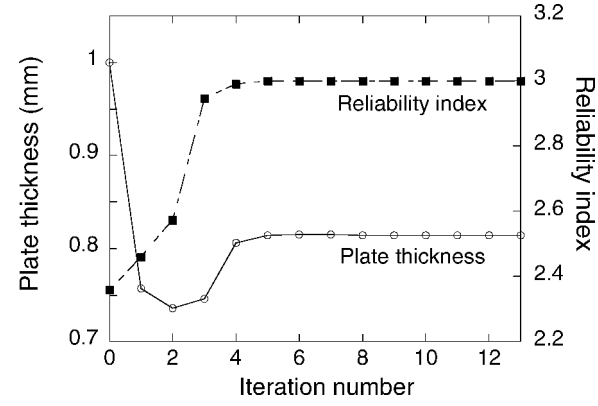

a) Plate thickness and reliability index

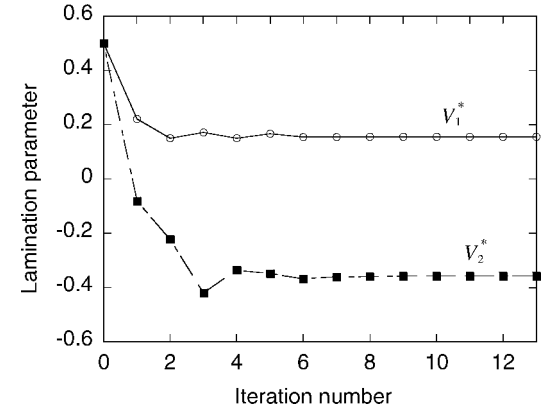

b) Lamination parameters

Fig. 9 Convergence history of the thickness-minimization design (load case 2).

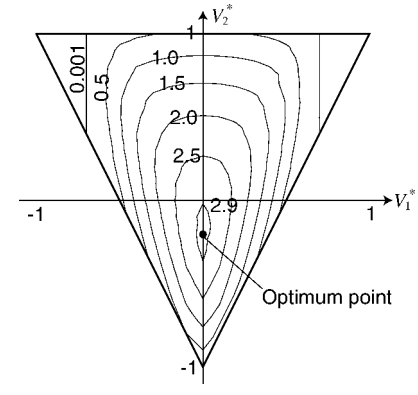

a) Load case 1

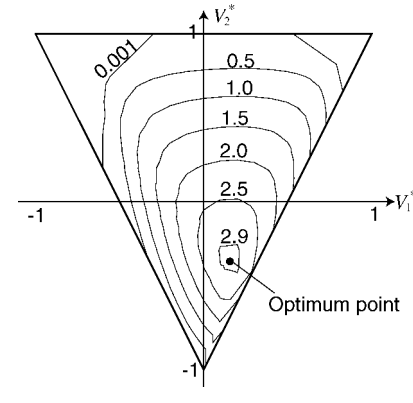

b) Load case 2

Fig. 10 Reliability index contours at the optimum thickness on the thickness-minimized design.

Conclusions

In this study, the lamination parameters are adopted as design variables for the reliability-based optimization of the laminated composite plate subject to in-plane loads. The reliability for the FPF criterion is evaluated by modeling the series system consisting of each ply failure. The mode reliability is evaluated by the FORM, where the material properties and applied loads are treated as random variables. Then the system reliability of the composite plate is evaluated by Ditlevsen's bounds.

Through numerical calculations, the following conclusions are remarked:

1) The reliability has a single peak and a continuous distribution in the lamination parameter space regardless of distribution types: normal, log-normal, and Weibull distributions.

2) The FORM is confirmed to have a sufficient accuracy for the reliability-based optimization in comparison with crude Monte Carlo simulation.

3) Consequently, adopting lamination parameters as design variables is considered a good strategy for the reliability-based optimization. This is demonstrated by the two types of reliability-based optimum design problem, that is, the reliability maximization of the constant-thickness plate and the thickness minimization under the reliability constraint.

The future problem is to apply the lamination parameters to other reliability-based design problems such as buckling reliability. Also, it is important that the proposed method be applied to the reliability-based design problem of a large composite structural system. Additionally, more efficient numerical strategies are required for the reliability analysis and the optimization.

Appendix: Tunneling Algorithms for FORM

It is necessary to obtain a global design point for accurate reliability evaluation by the FORM. For this purpose, the authors proposed to make use of the tunneling method,[13] which is known as one of the global optimization methods. The authors proposed a new tunneling function suitable for the FORM that includes the equality constraint of the FORM on the tunneling function.[12] Herein the tunneling method and the proposed tunneling function for the FORM are briefly described.

Tunneling Algorithm

The tunneling algorithm will find the global optimum point by iterating two phases: the minimization and the tunneling phases shown in Fig. A1. In the minimization phase, a local minimum $\boldsymbol{x}^*$ is searched by a conventional optimization method. The tunneling phase finds another point $\boldsymbol{x}^0$ that has the same value for the objective function as that of the local optimum but differs from the local point; $f(\boldsymbol{x}^0) = f(\boldsymbol{x}^*)$, $\boldsymbol{x}^0 \neq \boldsymbol{x}^*$. To move from $\boldsymbol{x}^*$, the tunneling function is defined by introducing a pole at the local optimum:

$$T(\boldsymbol{x}) = \frac{f(\boldsymbol{x}) - f(\boldsymbol{x}^*)}{[(\boldsymbol{x} - \boldsymbol{x}^*)^T(\boldsymbol{x} - \boldsymbol{x}^*)]^\lambda} \tag{A1}$$

where λ is a pole strength parameter. Another point $\boldsymbol{x}^0$ satisfies $T(\boldsymbol{x}^0) = 0$, but $\boldsymbol{x}^0 \neq \boldsymbol{x}^*$ is searched via a kind of Newton method. The name tunneling method comes from the process of finding $\boldsymbol{x}^0$ just like digging a tunnel under a mountain between $\boldsymbol{x}^0$ and $\boldsymbol{x}^*$.

The tunneling phase is started from the perturbed point from the local optimum:

$$\boldsymbol{x} = \boldsymbol{x}^* + \boldsymbol{\epsilon} \tag{A2}$$

where $\boldsymbol{\epsilon}$ is a random vector with $|\boldsymbol{\epsilon}| \ll 1$. The pole strength λ is determined so that the tunneling function will decrease as the point is moved away. When the point $\boldsymbol{x}^0$ satisfying $T(\boldsymbol{x}^0) = 0$ is found, the point is used as a starting point at the next minimization phase.

On the other hand, the minimization phase is converged to the point $\boldsymbol{x}_{T_{\text{opt}}}$ with $T(\boldsymbol{x}_{T_{\text{opt}}}) > 0$; the tunneling function is regarded as having a waving property. That is, the tunneling function has multiple local minima with positive values. In that case, the tunneling function is modified by introducing the movable pole at the local optimum points. Then the tunneling search is repeated until the zero point is found. The modified tunneling function is written in the following form:

$$T(\boldsymbol{x}) = \frac{f(\boldsymbol{x}) - f(\boldsymbol{x}^*)}{[(\boldsymbol{x} - \boldsymbol{x}^*)^T(\boldsymbol{x} - \boldsymbol{x}^*)]^\lambda [(\boldsymbol{x} - \boldsymbol{x}^m)^T(\boldsymbol{x} - \boldsymbol{x}^m)]^\eta} \tag{A3}$$

where $\boldsymbol{x}^m$ is a movable pole that is located at $\boldsymbol{x}_{T_{\text{opt}}}$ and η is the movable pole strength. Then the searching process is repeated to find the point $T(\boldsymbol{x}) < 0$. The starting point is randomly selected as follows:

$$\boldsymbol{x} = \boldsymbol{x}^m + \boldsymbol{\epsilon} \tag{A4}$$

If the point $\boldsymbol{x}^0$ satisfying $T(\boldsymbol{x}^0) = 0$ is found, the tunneling phase is finished and the point is used as a starting point for the next minimization phase. Otherwise, the tunneling search with the movable pole is repeated with a different initial point.

When the number of the search reaches the allowable limit, the tunneling phase is restarted from a new randomly selected point of Eq. (A2).

After several successive numbers, if the whole tunneling phase fails to find the better solution, the local optimum found in the previous minimization phase is regarded as the global optimum.[13]

An optimization algorithm can be adopted to find the minimum point of $T(\boldsymbol{x})$ instead of finding the zero point $T(\boldsymbol{x}) = 0$. When the point that satisfies the condition $T(\boldsymbol{x}) < 0$ is found during the optimization run, the minimization is broken off to start the next local minimization phase. The flow of the tunneling phase is illustrated in Fig. A2.

The concept of this algorithm is easily comprehended. However, the method is not widely applied to engineering design problems because of the difficulty of treating constraint conditions.[14]

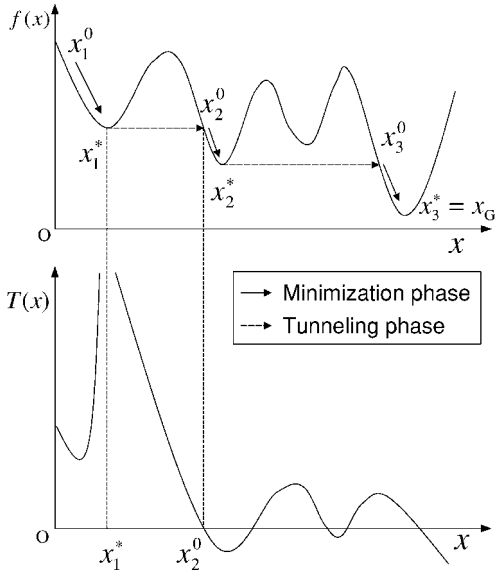

Fig. A1 Geometric interpretation of the tunneling algorithm and tunneling function.

Tunneling Function Suitable for FORM

It is difficult to directly apply the tunneling method to the FORM, because a limit state function must be treated as an equality constraint. To build in the constraint to the tunneling function (A1), the tunneling function is modified as follows:

$$T(\boldsymbol{u}) = f(\boldsymbol{u}) - f(\boldsymbol{u}^*) + \frac{\alpha[h(\boldsymbol{u})]^2}{[(\boldsymbol{u} - \boldsymbol{u}^*)^T(\boldsymbol{u} - \boldsymbol{u}^*)]^\lambda} \tag{A5}$$

where u^* denotes a local design point, $f(\boldsymbol{u})$ is the objective function defined as the square of the distance from the origin $f(\boldsymbol{u}) = \beta^2 = \boldsymbol{u}^T\boldsymbol{u}$, and α is a penalty parameter.

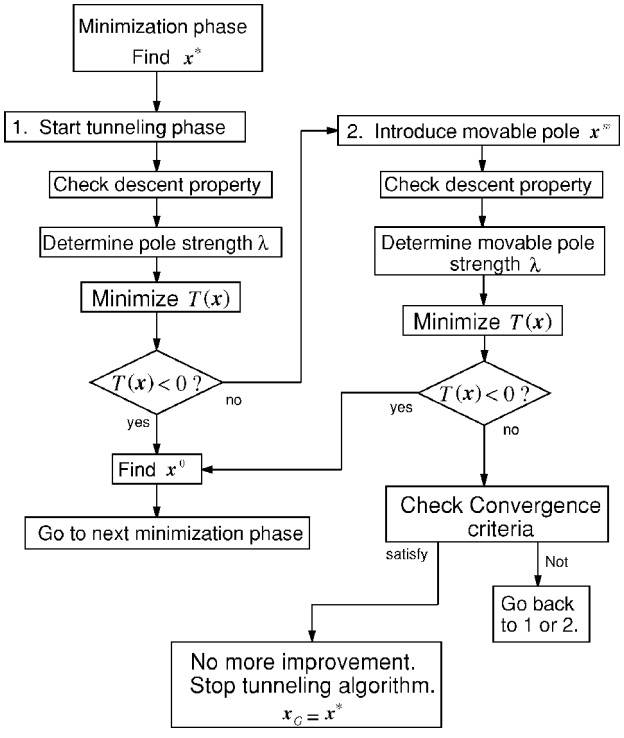

Fig. A2 Flowchart of the tunneling algorithm.

The penalty parameter is set as a multiplier of the limit state function value at the origin:

$$\alpha = k \cdot h(\mathbf{0}) \tag{A6}$$

where k is a positive number that is determined after some numerical experiments. Because the original objective function $f(\boldsymbol{u})$ has absolute minima at the origin $\boldsymbol{u} = \mathbf{0}$, the tunneling function should be sufficiently large at the origin.

In the tunneling phase, an optimization algorithm is adopted to find the minimum point of $T(\boldsymbol{u})$ instead of searching the zero point $T(\boldsymbol{u}) = 0$, $(\boldsymbol{u} \neq \boldsymbol{u}^*)$.

The tunneling function with movable pole (A3) is rewritten as follows:

$$T(\boldsymbol{u}) = f(\boldsymbol{u}) - f(\boldsymbol{u}^*) + \frac{\alpha[h(\boldsymbol{u})]^2}{[(\boldsymbol{u}-\boldsymbol{u}^*)^T(\boldsymbol{u}-\boldsymbol{u}^*)]^\lambda [(\boldsymbol{u}-\boldsymbol{u}^m)^T(\boldsymbol{u}-\boldsymbol{u}^m)]^\eta} \tag{A7}$$

Acknowledgment

The authors express their appreciation to H. Nakayasu for making valuable comments on this study.

References

[1]Gürdal, Z., Haftka, R. T., and Hajela, P., *Design and Optimization of Laminated Composite Materials*, Wiley, New York, 1999, pp. 138–153.

[2]Thoft-Christensen, P., and Murotsu, Y., *Application of Structural Systems Reliability Theory*, Springer-Verlag, Berlin, 1986, pp. 15–29.

[3]Miki, M., Murotsu, Y., Tanaka, T., and Shao, S., "Reliability of Unidirectional Fibrous Composites," *AIAA Journal*, Vol. 28, No. 11, 1990, pp. 1980–1986.

[4]Miki, M., Murotsu, Y., and Tanaka, T., "Optimum Fiber Angle of Unidirectional Composites for Load with Variations," *AIAA Journal*, Vol. 30, No. 1, 1992, pp. 189–196.

[5]Shao, S., Miki, M., and Murotsu, Y., "Optimum Fiber Orientation Angle of Multiaxially Laminated Composites Based on Reliability," *AIAA Journal*, Vol. 31, No. 5, 1993, pp. 919, 920.

[6]Miki, M., and Sugiyama, Y., "Optimum Design of Laminated Composite Plates Using Lamination Parameters," *AIAA Journal*, Vol. 31, No. 5, 1993, pp. 921–922.

[7]Todoroki, A., and Terada, Y., "Stacking Sequence Optimizations Using Fractal Branch and Bound Method," *Proceedings of the AIAA/ASME/ASCE/AHS/ASC 43rd Structures, Structural Dynamics, and Materials Conference* [CD-ROM], Paper 2002-1298, AIAA, Reston, VA, 2002.

[8]Miki, M., Murotsu, Y., Murayama, N., and Tanaka, T., "Application of Lamination Parameters to Reliability-Based Stiffness Design of Composites," *AIAA Journal*, Vol. 31, No. 10, 1993, pp. 1938–1945.

[9]Tsai, S. W., *Composites Design*, 4th ed., Think Composites, Dayton, OH, 1988, Sec. 11.

[10]Ditlevsen, O., "Narrow Reliability Bounds for Structural Systems," *Journal of Structural Mechanics*, Vol. 7, No. 4, 1979, pp. 453–472.

[11]Nakayasu, H., and Maekawa, Z., "A Comparative Study of Failure Criteria in Probabilistic Fields and Stochastic Failure Envelopes of Composite Materials," *Reliability Engineering and System Safety*, Vol. 56, No. 3, 1997, pp. 209–220.

[12]Kogiso, N., Nakagawa, S., and Murotsu, Y., "Application of Tunneling Algorithm to Reliability Analysis of Laminated Composite Plate," *Proceedings of the 9th IFIP Working Conference on Reliability and Optimization of Structural Systems*, edited by A. Nowak and M. Szerdesen, Univ. of Michigan, Ann Arbor, MI, 2001, pp. 135–142.

[13]Levy, A. V., and Montolvo, A., "The Tunneling Algorithm for the Global Minimization of Functions," *SIAM Journal on Scientific and Statistical Computing*, Vol. 6, No. 1, 1985, pp. 15–29.

[14]Chan, K. L., Kennedy, D., and Williams, F. W., "Hybrid Optimization Strategy Beyond Local Optima in Aerospace Panel Designs," *AIAA Journal*, Vol. 37, 1999, pp. 588–593.

A. Palazotto
Associate Editor